

The Imaging Fringe and Flexure Tracker of LINC-NIRVANA: Basic Opto-Mechanical Design and Principle of Operation

Christian Straubmeier^a, Thomas Bertram^a, Andreas Eckart^a, Steffen Rost^a, Yeping Wang^a,
Tom Herbst^b, Roberto Ragazzoni^c, and Gerd Weigelt^d

^a1. Physikalisches Institut, University of Cologne, Zùlpicher Str. 77, 50937 Cologne, Germany

^bMax-Planck-Institut für Astronomie, Königstuhl 17, 69117 Heidelberg, Germany

^cOsservatorio Astrofisico di Arcetri, L.go E. Fermi 5, 50125 Firenze, Italy

^dMax-Planck-Institut für Radioastronomie, Auf dem Hügel 69, 53121 Bonn, Germany

ABSTRACT

LINC-NIRVANA is the interferometric near-infrared imaging camera for the Large Binocular Telescope (LBT). Being able to observe at wavelength bands from J to K (supported by an adaptive optics system operating at visible light) LINC-NIRVANA will provide an unique and unprecedented combination of high angular resolution (~ 9 milliarcseconds at $1.25\mu\text{m}$), wide field of view (~ 100 arcseconds² at $1.25\mu\text{m}$), and large collecting area ($\sim 100\text{m}^2$).

One of the major contributions of the 1. Physikalisches Institut of the University of Cologne to this project is the development and provision of the Fringe and Flexure Tracking System (FFTS). In addition to the single-eye adaptive optics systems the FFTS is a crucial component to ensure a time-stable wavefront correction over the full aperture of the double-eye telescope, a mandatory pre-requisite for interferometric observations.

Using a independent HAWAII 1 detector array at a combined focus close to the science detector, the Fringe and Flexure Tracking System analyses the complex two-dimensional interferometric point spread function (PSF) of a suitably bright reference source at frame rates of up to several hundred Hertz. By fitting a parameterised theoretical model PSF to the preprocessed image-data the FFTS determines the amount of piston phase difference and angular misalignment between the wavefronts of the two optical paths of LINC-NIRVANA. For every exposure the corrective parameters are derived in real-time and transmitted to a dedicated piezo-electric fast linear mirror for simple path lengths adjustments, and/or to the adaptive optics systems of the single-eye telescopes for more complicated corrections.

In this paper we present the basic concept and current status of the opto-mechanical design of the Fringe and Flexure Tracker, the operating principle of the fringe and flexure tracking loops, and the encouraging result of a laboratory test of the piston control loop.

Keywords: LBT, LINC-NIRVANA, Fringe Tracking, Interferometry, Instrumentation

1. LINC-NIRVANA – THE NEAR-INFRARED INTERFEROMETRIC IMAGER FOR THE LARGE BINOCULAR TELESCOPE

Within the small group of large-scale interferometric near-infrared telescopes the Large Binocular Telescope (LBT) takes a unique position, since it is the only interferometer featuring a Fizeau-type optical layout with both primary mirrors sharing a common mount [Hill & Salinari 1998, 2004, Angel et al. 1998, Herbst & Hinz 2004].

At other (common) interferometers like VLTI* [von der Luehe et al. 1997, Glindemann et al. 2004] or the Keck Interferometer [Swanson et al. 1997, Colavita et al. 2004] the interferometric baselines are fixed with respect to the ground, since they are defined by the relative geographical locations of the individual telescopes. Therefore, while the pointing of the interferometer follows the apparent nightly motion of an observed astronomical source,

Send correspondence to C. Straubmeier: cstraubm@ph1.uni-koeln.de

*VLTI – Very Large Telescope Interferometer

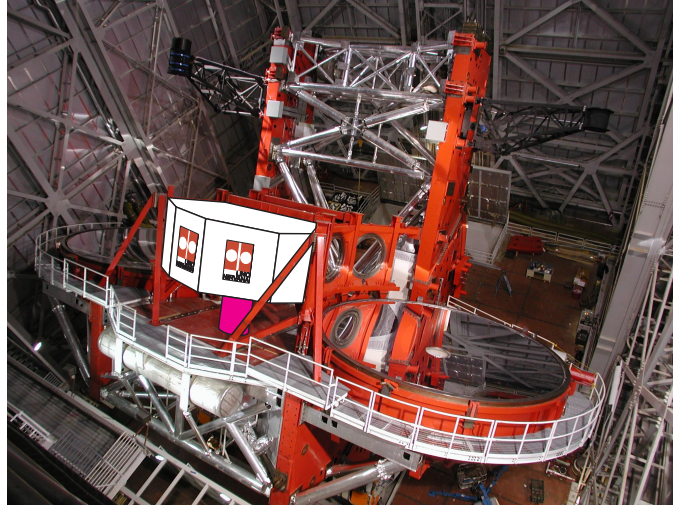


Figure 1. The image above shows the status of the Large Binocular Telescope (LBT) in January 2006 combined with a basic artist's impression of the LINC-NIRVANA system.

The telescope is already equipped with both 8.4m primary mirrors and both prime-focus spider-arms, with the spider-arm in the left hand side of the image carrying the first light camera LBC blue. Official *First Light* of the LBT using one primary mirror was achieved on October 12th, 2005, by taking a series of ten 30-second exposures of the galaxy NGC 891. For more information on the LBT, LBC, and the first light observations please refer to the articles of Hill et al. [2006], Hinz & Herbst [2006], and Ragazzoni et al. [2006] of this conference.

In the front of Fig. 1, on the platform inbetween the two primary mirrors, a sketch of the housing of LINC-NIRVANA has been added to the photo. LINC-NIRVANA is shown at its designated location at the *rear* (in the nomenclature of the LBT) bent foci of the interferometric platform, with the housing of the ambient temperature optics bench (carrying the collimators and the optics of the Multi-Conjugate Adaptive Optics (MCAO)) coloured white, and the 77K camera dewar (enclosing the beam combiner optics, the science camera and the Fringe and Flexure Tracker) underneath the bench coloured purple. To assess the impressive size of the instrument please compare its proportions to the diameter of the 8.4m primary mirrors. More information on the general design and status of LINC-NIRVANA can be found at Herbst et al. [2004] and Herbst et al. [2006].

the geometrical projection of the baseline onto the plane of the incoming wavefront (i.e. perpendicular to the line of sight) changes with time, giving rise to the need of technically challenging optical delay lines for path length compensation.

In contrast to that, the baseline of a Fizeau interferometer is not fixed with respect to the ground, but is fixed with respect to the steerable common central mount of the two mirrors. As a result, while tracking a celestial source, the length of the projection of the interferometric baseline of a Fizeau interferometer remains constant in time (at a length of the 14.4m for the case of the LBT), removing the necessity of complicated optical delay lines, and allowing for a much simpler and more compact instrument design. In addition, since the geometry of the entrance pupil of a Fizeau type interferometer is constant in time, too, it provides ideal premises for interferometric cameras featuring homothetic mapping (i.e. the output pupil is a scaled model of the input pupil), allowing for direct interferometric imaging over a (comparably) wide field of view [van Brug et al. 2004].

The LINC-NIRVANA near-infrared interferometric camera system, which is currently under construction by an international consortium of the Max-Planck-Institute for Astronomy (MPIA), the 1. Physikalisches Institut of the University of Cologne (Ph1), the Istituto Nazionale di Astrofisica of Italy (INAF), and the Max-Planck-Institute of Radioastronomy (MPIfR), is specifically tailored to exploit homothetic mapping (see Fig. 1 for an artist's impression of LINC-NIRVANA installed at the LBT). Using Multi-Conjugate Adaptive Optics (MCAO) [Berkefeld et al. 2001, Diolaiti et al. 2001, Ragazzoni et al. 2003, Arcidiacono et al. 2004] both single-eye input channels of LINC-NIRVANA will be operated close to the diffraction limit with significantly better (and larger) isoplanatism and higher sky-coverage than for the case of standard (i.e. non-MCAO) adaptive optics systems.

Operating at JHK bands (with the MCAO detectors sensing at visible wavelengths) LINC-NIRVANA will provide an unique and unprecedented combination of high angular resolution (~ 9 milliarcseconds at $1.25\mu\text{m}$ – defined by the linear separation of the two primary mirrors of 14.4m), wide interferometric field of view (~ 100 arcseconds² at $1.25\mu\text{m}$ – only limited by the physical size of the used HAWAII 2 detector array), and large collecting area ($\sim 100\text{m}^2$).

For an in-depth presentation and discussion of the overall design and functionality of the LINC-NIRVANA camera system please refer to Herbst et al. [2004, 2006].

2. FRINGE TRACKING – A MANDATORY ADAPTIVE OPTICS LOOP FOR INTERFEROMETRIC CAMERAS

In order to provide time-stable conditions for interferometric observations with long integration times (i.e. several seconds up to minutes) an interferometric beam-combiner must adhere to two fundamental physical properties at all times: all contributing telescopes must be operated at their diffraction limit (i.e. must provide undisturbed flat wavefronts), and all wavefront chunks of the individual telescopes must not show any phase deviation due to optical path length differences or atmospheric aberrations.

Since the first criterion applies to all (single-eye) ground based telescopes which shall deliver astronomical images of maximum angular resolution, it forms a well known and extensively studied requirement. Today's common approach for the diffraction limited operation of astronomical telescopes is the implementation of adaptive optics (AO) systems, i.e. deformable mirrors, wavefront sensors and fast numerical closed-loop algorithms, which correct the image degrading wavefront aberrations in real-time and in parallel to an ongoing exposure of the science detector. Besides of static or only slowly varying contributions from non-perfect telescope optics, most of these aberrations are due to the turbulent atmosphere of the earth with characteristic timescales of fractions of seconds to milliseconds. Although the correction gets technically more challenging with decreasing timescales, current generation AO systems can achieve loop frequencies of more than one hundred Hertz up to the kilohertz regime, and therefore be faster (or at least of the same order) than the characteristic timescale of atmospheric turbulence. As a consequence, the point spread function of an individual telescope can be brought close to its diffraction limit at most atmospheric conditions, what allows for long integration times of the science detector at the highest possible angular resolution of a single-eye telescope, and what forms the first step of wavefront correction for an interferometric camera like LINC-NIRVANA.

However, as mentioned before, an interferometric beam-combiner needs an additional second stage of wavefront correction, since even if the wavefronts from all contributing telescopes are corrected to perfection within their independent reference frames, there are still two aberrations left, which cannot be sensed and corrected by the AO systems of the individual telescopes:

- A fast varying part, which is due to large-scale atmospheric turbulence:
Since the adaptive optics systems of the individual telescopes sense and correct (i.e. flatten) the incoming disturbed wavefront only within their spatially separated single-eye apertures, a large-scale aberration (i.e. on spatial scales of the overall extent of the interferometer, which consists of several telescopes) manifests itself in a highly variable piston phase differences between the flat wavefront-chunks entering the beam-combiner from the individual telescopes (see Fig. 2).
- A constant or only slowly varying part, which may arise from mechanical flexure of the instrument (e.g. due to thermal changes or a changing direction of the vector of gravity as the telescope tracks a celestial source):
This flexure may result in changing optical path lengths of the two arms of the beam-combiner (once again resulting in a piston phase difference of the wavefronts at the combined focus), and/or lead towards a changing alignment of the optical axes of the system, i.e. the position of the different diffraction limited images of the single-eye telescopes will drift in the combined focal plane of the interferometer.

Both aberrations can obviously only be detected by a sensor at a combined focal plane of the interferometer, i.e. by a special Fringe and Flexure Tracker. Just as other (single-eye) aberrations, a non-perfect correction of either of both effects may reduce the fringe contrast of long integrated exposures of the science detector by up

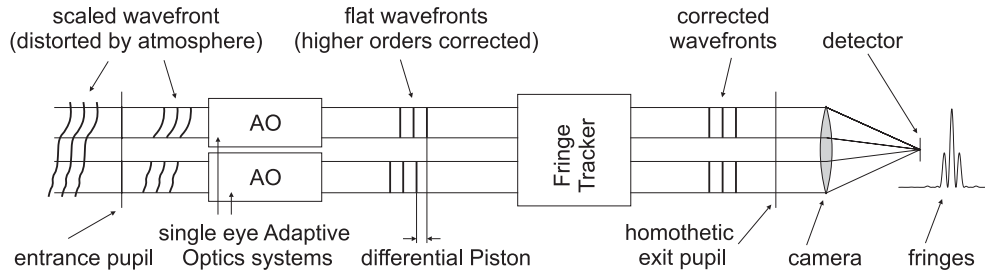


Figure 2. The diagram above illustrates the two consecutive steps of wavefront correction that have to be accomplished to allow for the time-stable operation of an interferometric camera system.

The left hand side of the image shows the incoming wavefront of the observed target just before it reaches the entrance pupil of an interferometric telescope. (For simplicity an interferometer of only 2 telescopes – i.e. one baseline – is shown. However, the presented scheme can be applied to cases of three or more telescopes, too, by increasing the number of single-eye adaptive optics systems respectively, with all single-eye channels still meeting at one fringe tracking unit.) Since the wavefront had to pass the turbulent atmosphere of the earth, the originally flat wavefront is severely distorted over a broad range of spatial frequencies, with the distortion being variable on sub-second timescales. Nevertheless, the wavefront does not exhibit any discontinuities in the mathematical sense before it passes the entry pupil of the interferometer. However, after the entry pupil (i.e. the spatially separated primary mirrors) several discrete pieces out of the formerly continuous wavefront are entering the beam-combiner optics.

In a first step, the discrete wavefront-chunks are corrected by common adaptive optics (AO) systems, i.e. the individual telescopes are operated as close to the diffraction limit as possible. But, since the single-eye AO systems are operating independently of each other, these devices are only sensitive to wavefront distortions within their own reference frame (i.e. the single-eye pupils). Therefore, the best correction that can be achieved by these systems will be discrete cuts of wavefronts, which are perfectly flat over the diameter of a single-eye pupil, but which will show a time dependent pistonic phase difference between each other. This low order aberration has to be corrected in a second step, and can only be measured by a sensor (i.e. a fringe tracker) at the combined focus of the interferometer, where it can observe the incoming wavefronts of all optical paths simultaneously. Based on the observed fringe pattern, the fringe tracker derives the amount of pistonic phase difference between the wavefront-chunks of the single-eye telescopes and introduces the respective corrective path length difference into the single-eye paths of the beam-combiner.

to 100% (depending on the remaining level of achieved correction), and therefore may preclude interferometric observations. In order to ensure a time-stable interferometric image quality and allow for deep integrations of the science detector, both aberrations have to be sensed and corrected in real-time and independently of any ongoing science observation. In the following sections of this article we will present the basic ideas of how this real-time correction will be realised at the LINC-NIRVANA interferometric near-infrared camera for the Large Binocular Telescope.

3. FFTS – THE FRINGE AND FLEXURE TRACKING SYSTEM OF LINC-NIRVANA

3.1. general design considerations

The general design and principle of operation of the Fringe and Flexure Tracking System (FFTS) of LINC-NIRVANA are based on the following list of specifications:

- Located at an interferometric focal plane of LINC-NIRVANA, the detector of the FFTS will sense those aberrations, which are not detectable by the Multi-Conjugate Adaptive Optics systems (MCAO) of the two single-eye telescopes. These two aberrations are a highly variable pistonic phase difference between the (MCAO corrected, i.e. flat) single-eye wavefronts entering the beam-combiner, and a slowly changing alignment of the optical axes of the two optical paths (see Sec. 2). All other (high order) aberrations of the wavefront from the observed source are assumed to be corrected to best extent by the MCAO systems of LINC-NIRVANA. The two incoming wavefronts sensed by the FFTS can therefore be assumed to be flat within their respective reference frames, i.e. they are free of higher order aberrations.

- Besides of slow changes of the optical path lengths within LINC-NIRVANA and the LBT (e.g. due to thermal gradients or mechanical flexure in response to a changing direction of the vector of gravity), most of the piston phase offset between the wavefronts of the two channels of the beam-combiner is introduced by the turbulent atmosphere of the earth. The characteristic timescale of these phase variations will therefore be tenth of seconds to milliseconds. The FFTS has to analyse and correct the phase offset in real-time in parallel (and independently) to an ongoing long term exposure of the science detector.
- Mechanical flexure within LINC-NIRVANA itself, as well as within the structure of LBT, and the instrument–telescope interface, may rise the need for continuous control of the alignment of the two optical axes of the beam-combiner in the interferometric focal plane. The characteristic timescale of alignment variations is expected to be tens of seconds or slower. The FFTS will determine possible misalignment on the appropriate time-scale and transmit the respective corrective parameters to the MCAO master control system.
- When the fringe tracking loop of the FFTS shall be closed after a longer period of time without continuous fringe tracking (e.g. at the begin of an observing night, or after a larger repointing of the telescope), the instrumental piston phase difference between the two optical paths of the beam-combiner has to be assumed unknown and may be off by several microns or more due to mechanical flexure and/or temperature gradients. The FFTS must be able to provide sufficient information to initialise the telescope–instrument assembly to zero optical path difference and well aligned optical axes in a sensible amount of time.
- In order to reduce potential non-common path aberrations, the detector of the FFTS shall be located at an interferometric focal plane close to the science detector.
- The detector of the FFTS shall be useable on reference stars in a field of view (FoV) as wide as possible, i.e. the usable FoV shall be limited by the isoplanatic image quality provided by the LINC-NIRVANA MCAO systems of the single-eye telescopes, and not by the physical size of the detector array of the FFTS.
- Similar to the science detector of LINC-NIRVANA, the FFTS shall operate at near-infrared JHK bands. Depending on the used wavelengths of the science observation the FFTS shall monitor adjacent bands.

In the following sections of this article we present a brief description of the optical & mechanical design, as well as the proposed sensing & analysing strategy of the Fringe and Flexure Tracker that result from the general design considerations listed above. For a more detailed discussion of the individual design issues we will give references to the respective other contributions of the Cologne FFTS working group to this conference.

3.2. optical design

According to the general design considerations listed in the previous section, the optical design of the Fringe and Flexure Tracking System (FFTS) of LINC-NIRVANA is based on a near-infrared HAWAII 1 detector array. This device features almost the same pixel size as the science detector (a significantly more expensive HAWAII 2 array), what allows to reduce the number of optical elements in the final non-common path to a minimum (since no refocussing optics to adapt different pixel scales are needed), and to position the detector of the FFTS quite close to the science detector. The optical paths towards the two detectors are split by an observer-selectable dichroic only about 100mm in front of the interferometric focal plane of LINC-NIRVANA, which reflects the selected J, H, or K-band onto the science detector while transmitting the respective other spectral bands towards the detector of the FFTS (see Fig. 3). The only optically active elements inbetween the separation point and the respective detector array are one filterwheel each, offering a variety of broad and narrow-band filters.

For an indepth discussion of the various aspects of the optical design of the entire interferometric LINC-NIRVANA camera system please refer to Bizenberger et al. [2006].

3.3. mechanical design

To maximise the sky-coverage of LINC-NIRVANA (i.e. the fraction of the sky that can be observed by the instrument with successfully closed adaptive optics and fringe tracking loops) the Fringe and Flexure Tracking System (FFTS) shall be able to lock on any suitable reference source around the science target within the

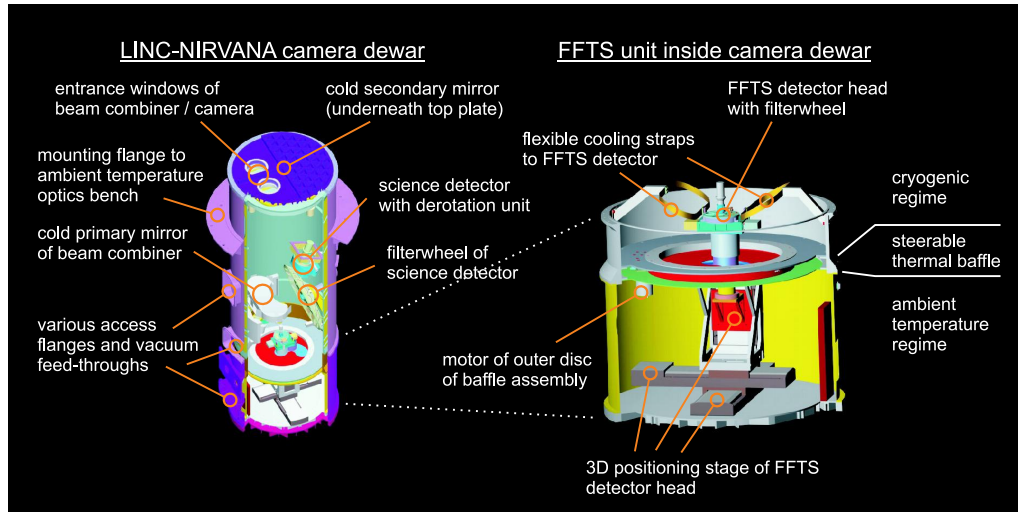


Figure 3. The figures above show CAD renderings of the 77K camera dewar of the LINC-NIRVANA beam-combiner (left) with special emphasis on the mechanical design of the Fringe and Flexure Tracking System (FFTS) at the bottom end of the dewar (right hand side enlargement).

The general design objective that the FFTS should be able to use any suitable reference source within the isoplanatic patch around the science target (see Sect. 3.1) requires the detector of the FFTS to be movable within a volume of $200 \times 300 \times 70 \text{ mm}^3$ (with the first two dimensions being defined by the assumed size of the isoplanatic patch provided by MCAO, and the third dimension arising from a curved focal plane). Since the movement has to be precise on sub-pixel (1pixel= $18.5\mu\text{m}$) level, a thorough investigation proved a pure cryogenic design of the positioning unit unsatisfactory (in terms of financial cost as well as guaranteed precision and reliability). As a result, a mixed temperature solution was chosen, with the linear positioning stages operating ambient temperature (although still located within the vacuum vessel of the cryostat) and only the attached detector head of the FFTS penetrating the cryogenic 77K volume of the cryostat. Although this solution demands an actively moved (and photon-proof) thermal baffle to create the sharp temperature transition, this approach is favoured for a variety of reasons (see Bertram et al. [2006b] for more details on the cryo-ambient mechanical design of the FFTS).

More information on the optical design of LINC-NIRVANA in general can be found at Bizenberger et al. [2006] and Laun et al. [2006] for the mechanical design of the NIR cryostat respectively.

isoplanatic patch provided by the Multi-Conjugate Adaptive Optics (MCAO) systems of the single-eye telescopes (see general design considerations in Sect. 3.1). At an assumed radius of the isoplanatic patch of about 30 to 45 arcseconds and a focal-ratio of LINC-NIRVANA of $\sim F/32$, this requires the detector of the FFTS to be movable within a volume of $200 \times 300 \times 70 \text{ mm}^3$, with an asymmetry of the xy-plane according to the elliptic extent of the focal plane of LINC-NIRVANA, and the third dimension compensating field curvature.

To realise this large positional freedom, the detector of the FFTS (including its readout electronics, temperature stabilisation, and spectral filterwheel) is mounted on a three-dimensional positioning device (see Fig. 3, [Bertram et al. 2006b]). Unfortunately, a suitable positioning stage has to satisfy tight mechanical constraints:

- The near-infrared detector array has to be operated at cryogenic temperature.
- The provided motion has to cover a large volume of $200 \times 300 \times 70 \text{ mm}^3$.
- After acquiring a suitable reference source away from the optical axis of LINC-NIRVANA, the detector has to track the position of this source continuously due to field rotation of the Alt.-Az. mount of the telescope.
- The achieved positional precision of the detector must be of sub-pixel scale (1pixel= $18.5\mu\text{m}$) while it tracks a celestial source, since the known centre of the Airy distribution is an important input parameter of the fringe tracking loop (see Sect. 3.4).

At first, prototypes of fully cryogenic designs got developed and evaluated in parallel at the local fine-mechanical workshop of the 1. Physikalisches Institut of the University of Cologne, and at specialised commercial companies. However, the local experiments on prototypes showed that while it is possible to achieve a reliable operation (i.e. there are no lock-ups), no prediction could be made whether the final devices would provide a positional repeatability of better than $10\mu\text{m}$ over a longer period of time (including multiple temperature cycles). Outsourcing the development to external companies failed for the same reason (possible contracts would not state a guaranteed precision) in addition to very high financial costs.

As a result, the mechanical design of the Fringe and Flexure Tracker was modified towards a semi-cryogenic concept (see Fig. 3). The changed design allows to use vacuum modified versions of commercial linear stages (which guarantee satisfying limits of mechanical tolerance, positional accuracy, positional repeatability, and tip-tilt-yaw) within their specified range of operating temperatures. In this scenario only a small platform carrying the near-infrared detector array, its readout electronics, and the filterwheel of the FFTS, is operated within the cryogenic volume of the camera dewar. While the semi-cryogenic concept simplifies the design of the mere positioning stage, it obviously requires a sophisticated actively controlled co-moving thermal baffle to tightly separate the ambient temperature regime of the linear stages from the cryogenic volume of the dewar, although providing a mechanical feed-through for the platform of the fringe tracking detector. However, since the motion of the positioning stage is known precisely well in advance (it is controlled and pre-programmed by the FFTS itself), the tolerance of the feed-through is of the order of millimetres, and the functionality of the thermal baffle can be based on rotation (a much easier movement in cryogenic environment), the feasibility, precision, and long-term reliability of the semi-cryogenic design variant is considered much higher than for a fully cryogenic setup. For more information on the cryo-ambient mechanical design of the FFTS please refer to [Bertram et al. 2006b].

3.4. closed-loop fringe tracking

The real-time piston control loop (i.e. the fringe tracking loop) of the FFTS uses a continuous rapid sequence of two-dimensional images of a reference source within the isoplanatic patch around the science target as input data. If the chosen source is bright enough, the input frame rate of the FFTS may be set to up to several hundred Hertz, with the maximum rate being a trade-off between a faster (and better) piston correction and a signal degrading increase in readout noise of the detector array. In presence of a bright enough reference source, the achievable image frequency can therefore be faster than the characteristic timescale of atmospheric turbulences at most atmospheric conditions.

After copying the data of the last exposure of the FFTS from a circular shared memory segment (where the taken frames are continuously stored by the readout electronics of the FFTS detector array) to a memory segment dedicated to the piston control loop, the first step towards a determination of the piston phase difference is to determine the centre of the 8.2m Airy distribution of the single-eye telescopes. Depending on the brightness of the monitored reference source (i.e. on the signal to noise ratio –SNR– of the image) two different scenarios are foreseen for that. In case of a bright source, the centre of the circular Airy distribution can be derived directly from the single frame by applying a two-dimensional numerical fit of a model Airy distribution (simply ignoring any interferometric modulation of the observed intensity distribution). For fainter sources and a SNR too low to achieve a satisfying quality of the numerical fit, the centre of the Airy distribution can be provided by the flexure control loop of the FFTS. Operating on a much slower characteristic timescale (i.e. being able to sum up several individual low SNR images), the flexure control loop is able to determine the centre of the Airy distribution with high precision even on fainter reference sources (see Sect. 3.6).

As a second step the central rectangle of the 2-D image is vertically collapsed (by averaging or taking a median) delivering an intensity profile along the horizontal interferometric axis of the image (see Fig. 4). The vertical position of this rectangle is centered on the previously derived vertical centre of the Airy distribution, and the height of the box is chosen by the fringe tracking loop in a way to obtain a maximum SNR of the resulting horizontal line profile (the width of the box is set to the full width of the 2-D image).

In a third and final step of image analysis, the piston control loop fits a parameterised model of the one-dimensional interferometric intensity distribution of LINC-NIRVANA to the observed line profile (see Fig. 4). Based on fixed and known optical parameters (i.e. the 8.2m single-eye apertures, the 14.4m interferometric

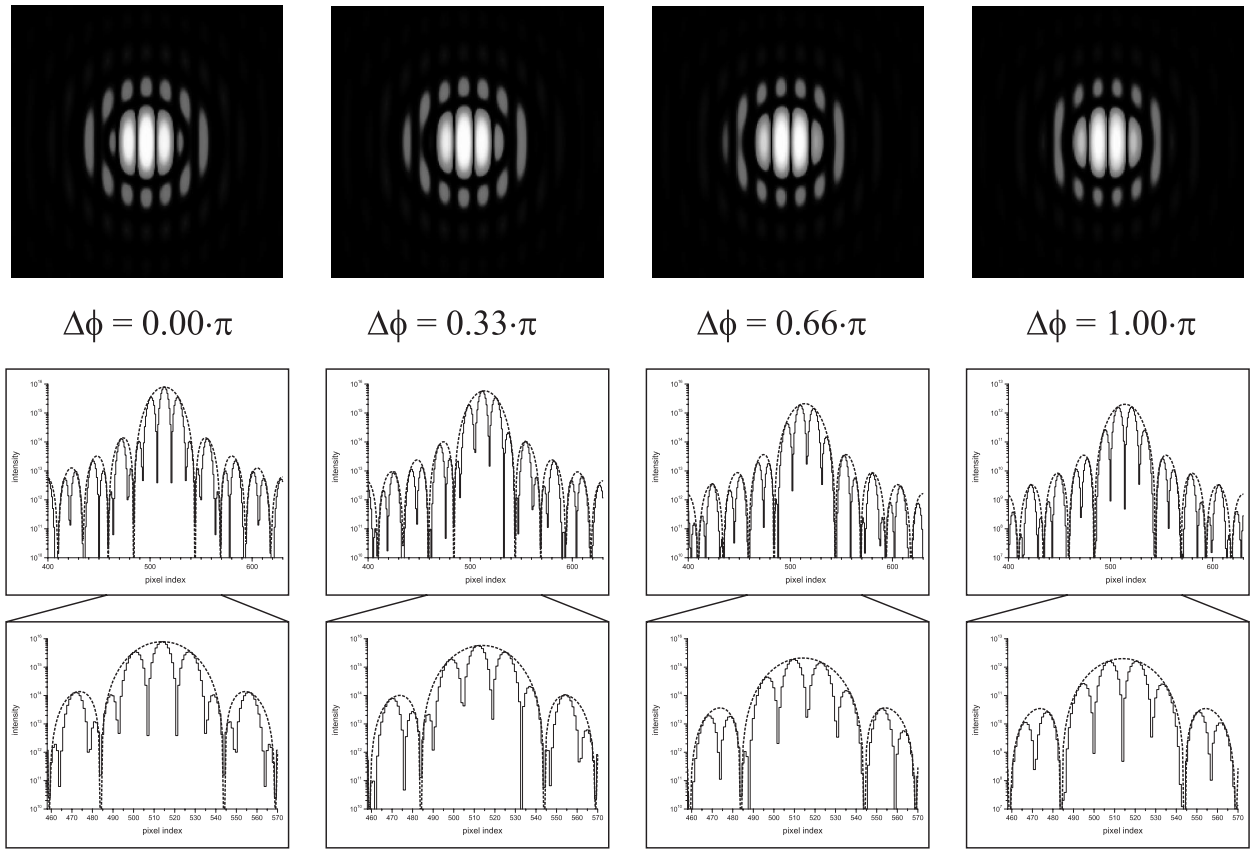


Figure 4. The figure above presents the result of numerical simulations of the monochromatic interferometric point spread function (PSF) of LINC-NIRVANA under the assumption of different values of piston phase difference (from left to right $\Delta\phi = 0.00\pi, 0.33\pi, 0.66\pi$ & 1.00π respectively) inbetween the perfectly MCAO corrected (i.e. flat) wavefronts from the two single-eye telescopes. The simulation is based on a single-eye aperture of 8.2 metres and an interferometric baseline of 14.4 metres.

The upper row of images shows the two-dimensional intensity distribution of a bright reference source (using a logarithmic colour map) like it is observed by the imaging detector of the Fringe and Flexure Tracker (for presentation purposes the pixel resolution of the images is higher than the real pixel scale). Although the graphical representation of the huge intensity differences of the individual maxima of more than four orders of magnitude can be only partially successful, the images give a fine impression of how the interferometric PSF of LINC-NIRVANA is combined from the superposition of the circular Airy distribution of the individual 8.2m telescopes, and the interferometric *cos*-based variation of the 14.4m baseline along the horizontal axis of the image [Bertram et al. 2006a].

The middle and lower rows of images display linear intensity profiles (using arbitrary units) along the horizontal (i.e. interferometric) axes of the 2-D images, with the lower row showing the central regions of the PSF only. While the stepped curves represent the actual data of the numerical simulations, the dashed lines indicate the Airy distribution of a 8.2m aperture in absence of interferometric modulation (e.g. perpendicular to the interferometric baseline, or after a loss of coherence).

Comparing the images from left to right (i.e. in direction of increasing piston phase difference) one can see how the sinusoidal interferometric intensity modulation shifts along the horizontal axis with respect to the centre of the Airy distribution. For the case of no piston phase difference (left hand side images) the centre of the 0th order (i.e. white) fringe coincides with the Airy centre, while for the case of 1.00π of differential piston (right hand side images) the first interferometric minimum is located at that position.

By the analysis of the intensity line profile and the offset of the interferometric intensity modulation with respect to the centre of the underlying Airy distribution it is therefore possible to derive the amount of piston phase difference that was present at the time of the exposure (please refer to Bertram et al. [2006a] for more information on the image analysis concept of the Fringe and Flexure Tracker of LINC-NIRVANA).

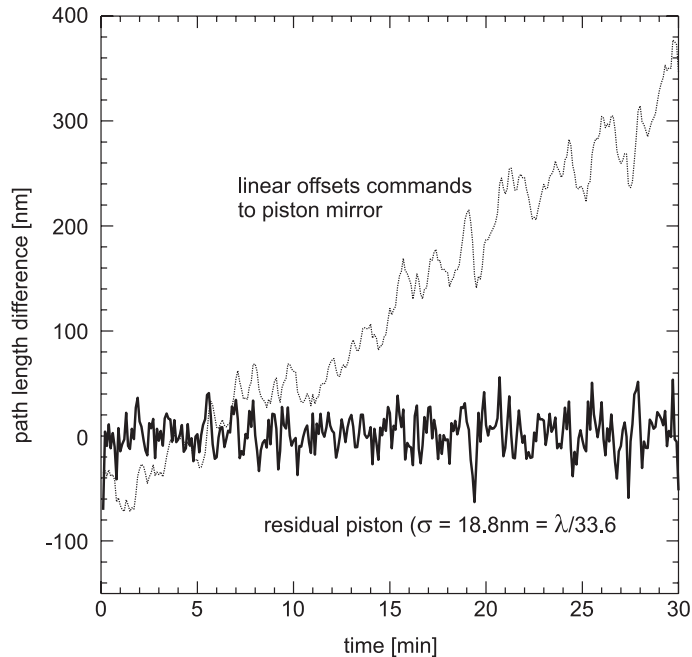


Figure 5. Using the LINC-NIRVANA testbed Fizeau interferometer, a 1:3 scale model setup of the final LINC-NIRVANA interferometer, with a diode laser ($\lambda \sim 670\text{nm}$, coherence length $\sim 0.2\text{mm}$) and an optical CCD detector, it was possible to test a first prototype of the planned fringe tracking loop on real hardware and study the temporal evolution of pistonic aberrations in a controlled laboratory setup [Andersen et al. 2004] at the Max-Planck-Institute for Astronomy. Although the used hardware limited the maximum loop frequency to a very low value of $\sim 0.2\text{Hz}$ it was possible to stabilise the optical path length difference over 30 minutes to better than $\lambda/30$ while compensating about $1\mu\text{m}$ of pistonic aberration arising from temperature changes of the laboratory. (Note: The figure on the left plots linear offsets of the piston mirror which are half of the resulting change in optical path length.)

baseline, and the centre of the Airy distribution) the theoretical model depends on only two parameters: the amount of pistonic phase difference between the wavefronts of the two single-eye telescopes, and the overall intensity of the reference source.

After applying a suitable gain parameter to avoid unwanted resonance frequencies and overshoot the derived corrective change of optical path length to stabilise the fringe pattern is transmitted to the control electronics of the piston mirror of the ambient temperature optics of LINC-NIRVANA (in presence of large corrections the fringe control loop might also ask the single-eye MCAO systems of LINC-NIRVANA for slow pistonic adjustments in order to keep the piezoelectric fast piston mirror within its dynamic range).

For more information on the image analysis concept and the anticipated performance of the Fringe and Flexure Tracker of LINC-NIRVANA please refer to Bertram et al. [2006a]. Details of the planned piston control strategies are given in Rost et al. [2006], and the used Linux based real-time computing environment of the FFTS is described in Wang et al. [2006].

To get a first impression of the performance of this piston control concept in cooperation with real hardware (complementary to extensive numerical simulations using artificially generated input data and comparing the derived correction to the known input signal [Bertram et al. 2006a]), the fringe tracking loop described above was tested on the LINC-NIRVANA testbed Fizeau interferometer [Andersen et al. 2004], a 1:3 scale model setup of the beam-combiner optics of LINC-NIRVANA at the Max-Planck-Institute for Astronomy. The result of this experiment is shown in Fig. 5, and although the maximum possible loop frequency was below 1Hz (due to limitations of the used off-the-shelf computing environment and low-bandwidth/high-latency hardware controllers), the achieved pistonic correction was better than $\lambda/30$ over a time of more than 30 minutes, while the piston control loop successfully compensated about $1\mu\text{m}$ of accumulated change in optical path length of the two paths of the testbed interferometer.

In order to extend the laboratory tests of the piston control concept and to get the parameters of the tests to more realistic values the 1. Physikalisches Institut of the University of Cologne is currently building a dedicated new interferometric test setup in its local laboratories. The piston control loop of this new testbed will be able to operate at loop frequencies of several hundred Hertz, and the setup will allow to introduce precisely known optical path differences (OPD) independently of the fringe tracking loop (to simulate atmospheric aberration) at a rate of several hundred Hertz, too. It will therefore be possible to analyse the achieved quality of correction of the fringe tracking loop by comparing the derived value of pistonic aberration of the FFTS with the known

value of introduced OPD. The experiment will deliver valuable data to check and calibrate the results of the extensive numerical simulations of the performance of the FFTS done in the last years.

3.5. variable bandwidth operation and pistonic system alignment

In addition to the closed-loop piston control described in the previous section, the Fringe and Flexure Tracking System (FFTS) is also an important component for the initial setup and alignment of the LINC-NIRVANA instrument and the instrument–telescope assembly. After the fringe tracking loop has been open for a longer period of time (e.g. at the begin of an observing night, or after a larger slew of the telescope) the pistonic difference between the two optical paths of the LINC-NIRVANA–LBT assembly is unknown and may be of several several micron or more due to mechanical flexure and/or temperature gradients. At such conditions the optical paths of the LINC-NIRVANA–telescope system have to be initialised to zero instrumental OPD, i.e. a large range of pistonic phase offsets must be scanned to look for the 0th order fringe of a bright reference source. Assuming a successful operation of the adaptive optics systems of the single-eye telescopes (a mandatory condition for all tasks of the FFTS) this instrument alignment will be controlled by the FFTS, too.

To illustrate this functionality Fig. 6 shows two sets of numerically simulated point spread functions (PSF) of LINC-NIRVANA, with the images of each set being based on three different spectral bandwidths (i.e. $\Delta\lambda = 1\%$, 16% & 46% from left to right), and the two sets marking the cases of zero OPD (left hand set) and $\Delta\phi = 2.50\mu\text{m}$ (right hand set). Comparing the three images of each set it can be seen how the coherence length decreases with increasing spectral bandwidth, reducing the intensity contrast of higher order fringes and accentuating the 0th order (white) fringe. A large spectral bandwidth configuration of FFTS will be chosen for closed-loop piston control since it provides maximum flux (i.e. signal) of the reference source (enabling high loop frequencies) and allows to identify the 0th order fringe of zero phase difference most easily and unambiguously.

However, if the OPD of the instrument–telescope assembly is very large (i.e. the fringe tracking loop was not active for some time and the system lost its pistonic alignment), the broadband PSF of a reference source may show no detectable interferometric intensity modulation at all. In such cases, FFTS will be configured for smaller spectral bandwidth (by switching filters of its filterwheel) to increase the intensity contrast of higher order fringes. Operating a lower loop frequencies (to compensate the reduced narrowband flux of the reference source) FFTS will then be able to analyse the intensity modulation of the higher order fringes to determine the direction of correction towards zero OPD (the fringe contrast increases with decreasing order). Since the corrective range of the fast piezoelectric piston mirror is limited, requests for larger changes of OPD will be transmitted to the adaptive optics systems of LINC-NIRVANA, which will use its deformable mirrors or the adaptive secondaries of the telescope. Approaching the vicinity of zero OPD, FFTS will gradually increase the spectral bandwidth to allow for higher loop frequencies, better quality of correction, and firm identification of the 0th order fringe.

3.6. flexure control

Besides of the control of pistonic phase differences between the two optical paths of LINC-NIRVANA, the Fringe and Flexure Tracking System has to monitor and control the proper alignment of the optical axes of the two paths. Similar to the piston control this task can only be accomplished by a detector system at the combined focal plane of the beam-combiner.

This flexure control loop (named after the presumed primary source of changing alignment) uses the same continuous flow of two-dimensional images that also serve the fringe tracking loop, however, it applies a different analysis to derive the position of the optical axes of the two optical paths. While the fringe tracking loop analyses the interferometric intensity modulation of the observed point spread function along the horizontal axis of the images, the analysis of the flexure control loop is based on the circular Airy pattern of the 8.2m primary mirrors.

The Airy pattern is clearly visible in the simulated data of Fig. 4 and Fig. 6, but as can be seen directly in the lower linear intensity plots of Fig. 4, the maximum intensity of the first Airy ring is already about two orders of magnitudes fainter than the maximum intensity of the central fringe. Taking into account that the exposure time of the frames will be set as short as possible in order to obtain high loop frequencies of the piston control loop (and therefore a good correction of the fast varying atmospheric pistonic aberration), the signal to noise ratio (SNR) of the images will be too low to detect the location of the faint Airy maxima with satisfying precision on

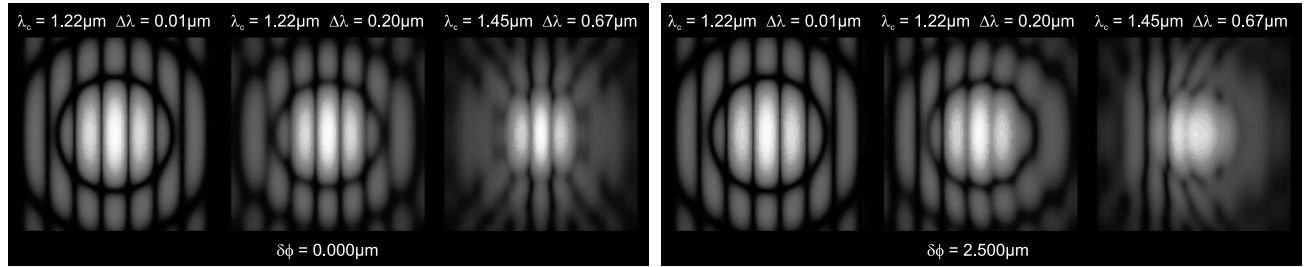


Figure 6. The two sets of images above visualise the results of numerical simulations of the interferometric point spread function (PSF) of LINC-NIRVANA with each set featuring three different spectral bandwidths (i.e. $\Delta\lambda = 1\%$, 16% & 46%), and with the left set showing the results for zero phase difference between the two wavefronts (i.e. the 0^{th} order fringe is located in the middle of the image) and the right one being based on a phase difference of $\Delta\phi = 2.50\mu m$ (i.e. the white fringe is offset about two maxima to the left hand side of the image).

Comparing the respective images of each set from left to right (i.e. in the direction of broader spectral bandwidth) it becomes increasingly easier to unambiguously identify the 0^{th} order (i.e. white) fringe, which denotes the angular position of no piston phase difference. The identification (as well as its designation as 'white') is based on the physical fact, that only for this fringe the intensity maxima of all wavelengths are located at the same position on the detector, i.e. the angular position of the fringe is achromatic. Since for a limited spectral bandwidth the condition of achromatism holds true (at least to first order) for the 1^{st} intensity minima, too, the 0^{th} order fringe is characterised by the fact that this fringe is showing the maximum intensity contrast (which may be close to 100% in absence of higher order aberrations) between its maximum and its adjacent minima. While in the case of small spectral bandwidth (left hand side images of each set) the condition of achromatism holds true for the next higher order fringes, too, the higher order fringes increasingly lose fringe contrast at broader bandwidths (middle and right hand side images of each set).

the basis of individual frames. Fortunately, the characteristic timescale of instrumental flexure (which should be the only reason of changing alignment of the optical axes, since all similar high order atmospheric aberrations like tip & tilt get corrected by the adaptive optics systems of the single-eye telescopes) is much slower than the sub-second timescale of atmospheric aberrations.

Due to this relaxed timescale the flexure control loop will be able to numerically sum up several hundreds or thousands of individual low SNR frames to create a "long exposure" image, which will be "deep" enough to assess the faint two-dimensional Airy pattern. The analysis will fit a parameterised model intensity distribution to this image, in order to derive a potential decorrelation of the Airy patterns of the two single-eye telescopes. While a potential correction of the optical axes will be transmitted to the single-eye adaptive optics systems of LINC-NIRVANA, the precise sub-pixel knowledge of the location of the centre of the Airy pattern will also serve as an important input parameter of the fringe tracking loop (see Sect. 3.4).

4. SUMMARY

The Fringe and Flexure Tracking System (FFTS) developed at the 1. Physikalisches Institut of the University of Cologne is an elementary component for the proper interferometric operation of the LINC-NIRVANA near-infrared camera for the Large Binocular Telescope.

The development is split in two work packages: the design and construction of the partially cryogenic movable mechanical structures of the device (i.e. the three-dimensional positioning stage of the near-infrared detector array and the cryo–ambient thermal baffle), and the design and implementation of the closed-loop analysis algorithms for piston and flexure control.

As presented in this paper there is satisfying progress on both fields, with respect to the general schedule of LINC-NIRVANA. The current hardware design features a cryo–ambient transition, what allows to use commercial (ambient temperature) high precision linear stages, while keeping the detector array of FFTS at temperatures of liquid nitrogen. A first prototype of the fringe tracking loop achieved an encouraging quality of fringe stabilisation in a laboratory test at the LINC-NIRVANA testbed Fizeau interferometer.

ACKNOWLEDGMENTS

This work is supported in parts by the Deutsche Forschungsgemeinschaft (DFG) via grants SFB 494, HBF 111-519 & #111-520, and Verbundforschung 05AL2PLA/5 & 05AL5PKA/0.

REFERENCES

- Andersen, D. R., Bertram, T., Bizenberger, P., et al. 2004, in *New Frontiers in Stellar Interferometry*, Proceedings of SPIE Volume 5491. Edited by Wesley A. Traub. Bellingham, WA: The International Society for Optical Engineering, 2004., p.1760, ed. W. A. Traub, 1760–+
- Angel, J. R. P., Hill, J. M., Strittmatter, P. A., Salinari, P., & Weigelt, G. 1998, in *Proc. SPIE Vol. 3350*, p. 881-889, *Astronomical Interferometry*, Robert D. Reasenberg; Ed., 881–889
- Arcidiacono, C., Diolaiti, E., Ragazzoni, R., Farinato, J., & Vernet-Viard, E. 2004, in *Advancements in Adaptive Optics*. Edited by Domenico B. Calia, Brent L. Ellerbroek, and Roberto Ragazzoni. Proceedings of the SPIE, Volume 5490, pp. 563-573 (2004)., ed. D. Bonaccini Calia, B. L. Ellerbroek, & R. Ragazzoni, 563–573
- Berkefeld, T., Glindemann, A., & Hippler, S. 2001, *Experimental Astronomy*, 11, 1
- Bertram, T., Arcidiacono, C., Straubmeier, C., et al. 2006a, in *Proc. SPIE Vol. 6268*, *Advances in Stellar Interferometry*
- Bertram, T., Baumeister, H., Straubmeier, C., et al. 2006b, in *Proc. SPIE Vol. 6268*, *Advances in Stellar Interferometry*
- Bizenberger, P., Diolaiti, E., Egner, S. E., et al. 2006, in *Proc. SPIE Vol. 6269*, *Ground-Based and Airborne Instrumentation for Astronomy*
- Colavita, M. M., Wizinowich, P. L., & Akeson, R. L. 2004, in *New Frontiers in Stellar Interferometry*, Proceedings of SPIE Volume 5491. Edited by Wesley A. Traub. Bellingham, WA: The International Society for Optical Engineering, 2004., p.454, ed. W. A. Traub, 454–+
- Diolaiti, E., Ragazzoni, R., & Tordi, M. 2001, *Astron. & Astroph.*, 372, 710
- Glindemann, A., Albersen, M., Andolfato, L., et al. 2004, in *New Frontiers in Stellar Interferometry*, Proceedings of SPIE Volume 5491. Edited by Wesley A. Traub. Bellingham, WA: The International Society for Optical Engineering, 2004., p.447, ed. W. A. Traub, 447–+
- Herbst, T. M., Eckart, A., Ragazzoni, R., & Weigelt, G. P. 2006, in *Proc. SPIE Vol. 6268*, *Advances in Stellar Interferometry*
- Herbst, T. M. & Hinz, P. M. 2004, in *New Frontiers in Stellar Interferometry*, Proceedings of SPIE Volume 5491. Edited by Wesley A. Traub. Bellingham, WA: The International Society for Optical Engineering, 2004., p.383, ed. W. A. Traub, 383–+
- Herbst, T. M., Ragazzoni, R., Eckart, A., & Weigelt, G. 2004, in *Ground-based Instrumentation for Astronomy*. Edited by Alan F. M. Moorwood and Iye Masanori. Proceedings of the SPIE, Volume 5492, pp. 1045-1052 (2004)., ed. A. F. M. Moorwood & M. Iye, 1045–1052
- Hill, J. M., Green, R. F., & Slagle, J. H. 2006, in *Proc. SPIE Vol. 6267*, *Ground-Based and Airborne Telescopes*
- Hill, J. M. & Salinari, P. 1998, in *Proc. SPIE Vol. 3352*, p. 23-33, *Advanced Technology Optical/IR Telescopes VI*, Larry M. Stepp; Ed., 23–33
- Hill, J. M. & Salinari, P. 2004, in *Proceedings of the SPIE*, Volume 5489, pp. 603-614 (2004)., ed. J. M. Oschmann, 603–614
- Hinz, P. M. & Herbst, T. 2006, in *Proc. SPIE Vol. 6268*, *Advances in Stellar Interferometry*
- Laun, W., Baumeister, H., & Bizenberger, P. 2006, in *Proc. SPIE Vol. 6269*, *Ground-Based and Airborne Instrumentation for Astronomy*
- Ragazzoni, R., Giallongo, E., Pasian, F., et al. 2006, in *Proc. SPIE Vol. 6267*, *Ground-Based and Airborne Telescopes*
- Ragazzoni, R., Soci, R., Arcidiacono, C., et al. 2003, in *Astronomical Adaptive Optics Systems and Applications*. Edited by Tyson, Robert K.; Lloyd-Hart, Michael. Proceedings of the SPIE, Volume 5169, pp. 181-189 (2003)., ed. R. K. Tyson & M. Lloyd-Hart, 181–189
- Rost, S., Bertram, T., Straubmeier, C., Wang, Y., & Eckart, A. 2006, in *Proc. SPIE Vol. 6274*, *Advanced Software and Control for Astronomy*
- Swanson, P., Colavita, M., Boden, A., van Belle, G., & Shao, M. 1997, *Bulletin of the American Astronomical Society*, 30, 756
- van Brug, H., Oostdijck, B., Snijders, B., van der Avoort, C., & Gori, P.-M. 2004, in *New Frontiers in Stellar Interferometry*, Proceedings of SPIE Volume 5491. Edited by Wesley A. Traub. Bellingham, WA: The International Society for Optical Engineering, 2004., p.1598, ed. W. A. Traub, 1598–+
- von der Luehe, O., Derie, F., Koehler, B., et al. 1997, in *Proc. SPIE Vol. 2871*, p. 498-503, *Optical Telescopes of Today and Tomorrow*, Arne L. Ardeberg; Ed., 498–503
- Wang, Y., Bertram, T., Rost, S., Straubmeier, C., & Eckart, A. 2006, in *Proc. SPIE Vol. 6274*, *Advanced Software and Control for Astronomy*